Cross Flow Investigation by Stereoscopic PIV measurements

L. David[(1)], R. Fraticelli, D. Calluaud, J. Borée

Laboratoire d'Études Aérodynamiques (UMR 6609-CNRS)
Boulevard Pierre et Marie Curie Téléport 2, B.P. 30179
86960 FUTUROSCOPE POITIERS Cedex, FRANCE
(1) Laurent.David@univ-poitiers.fr

Abstract

In this paper, first results of the study of perpendicular fluid injection through a square hole in a cross flow are presented. From Stereoscopic Particle Image Velocimetry measurements in different sections, the average and instantaneous velocity fields allow to characterize the main aspect of the flow for a Reynolds number of 770 and different injection velocity rates lower than 0.65.

The existence of shear-layer vortices, counter-rotating vortex pair, horseshoe and wake vortices is showed for the highest jet velocity and some of them disappear when the injection rate decreases. Most of new information appears in the cross-section downstream the jet. The well known kidney vortex appears unsteady and composed for τ_{inj}=0.63 by two counter-rotating vortex pairs which merge at the frequency of the shedding of the shear-layer vortices. For the two other injection rates, only one CVP exists and moves for τ_{inj}=0.31 in a spiral rollup. These phenomena are identical to those found by Haven and Kurosaka (1997).

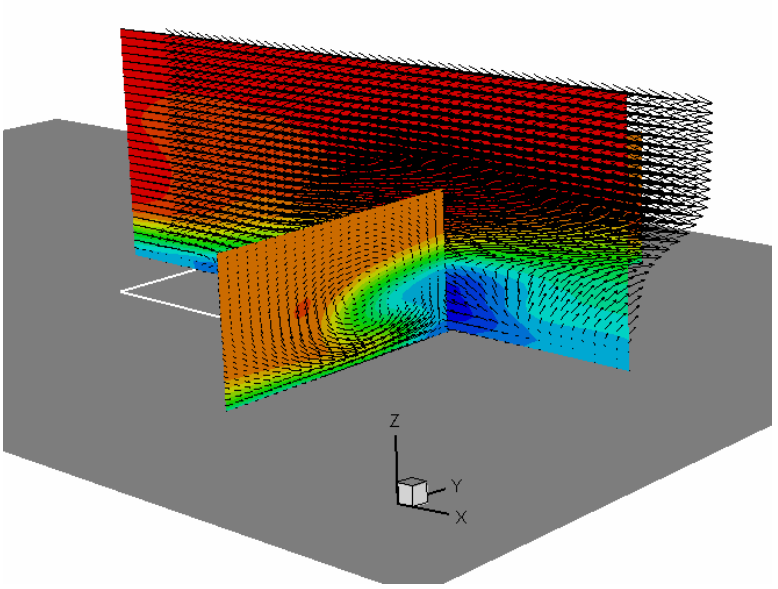

Cross-flow 3C PIV measurements

1. Introduction

The interaction of a jet and a cross flow has been the subject of much investigation for over seventy years and has significance in many practical applications including combustion, pollution transport and industrial mixing. Several parameters such Reynolds number, ratio of jet flow to cross flow momentum, jet shape, influence and modify the mixing of the jet, the existence of shear-layer vortices, counter-rotating vortex pair, horseshoe and wake vortices (Andreopoulos and Rodi, 1984) (Fric and Roshko, 1994). Haven and Kurosaka (1997) have shown the effect of the hole shape on the kidney vortices for Reynolds number around 1000 and the presence of two pairs of counter-rotating vortex for a square injection.

In microgravity conditions, diffusion flames are strongly conditioned by the aerodynamic fields of the fuel injected to a stream of oxidiser flowing parallel to the square burner (Brahmi et al., 2004). In a first simplified approach, the interactions between two fluids with same density are investigated for low Reynolds number (Re=770) and jet-to-cross flow velocity ratio lower or equal to 0.63. The steady and unsteady behaviour of the flow, the main 3D vortices and the mixing flow are characterized and compared by visualizations and Stereoscopic Particle Image Velocimetry for different velocity ratio in different sections. The influence of the ratio of jet flow to cross flow velocity is presented in details and modifies strongly the development of the counter-rotating vortex pair.

2. Experimental devices

The jet in a cross-flow under investigation is created in a closed-circuit hydrodynamic channel. The layout of the test section is shown in Figure 1, where the injection length is D=30mm. A smooth, wedge shaped false bottom has been fixed in the test section with the injection emanating from the hole in it to control the thickness of the boundary layer.

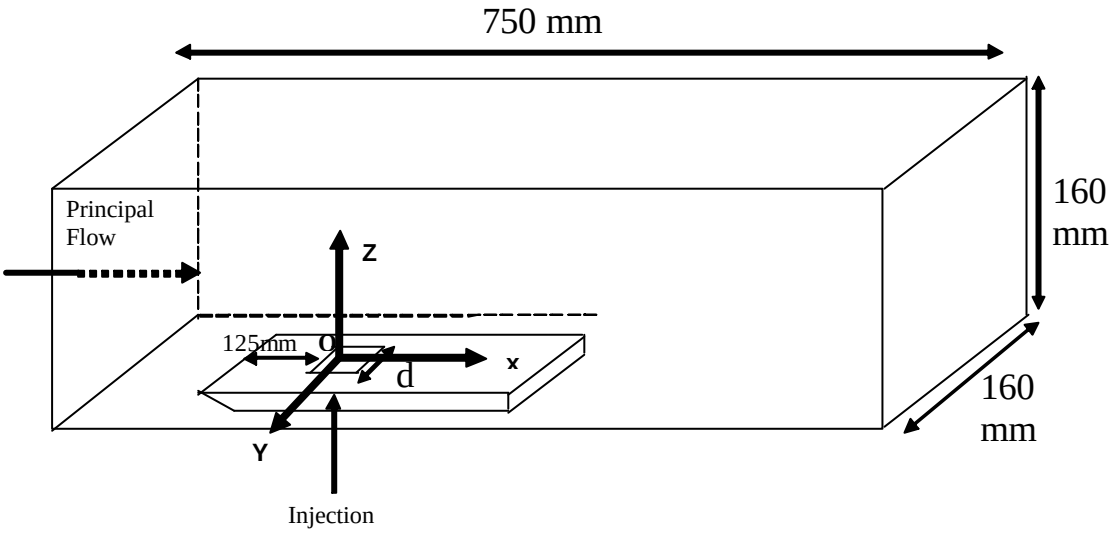

Fig. 1 – Test section dimensions and axes system.

The Reynolds number 770 of the main flow is calculated with the characteristic length of the square injection orifice D, principal flow speed U_∞ and kinematics viscosity of water. Three injection ratios t_{inj} (defined by the ratio between the jet velocity and the main flow velocity) lower than 1 (0.63, 0.31, 0.15) have been investigated.

Six sections of the flow (Y/D=0,1/6,1/3, ½ and X/D=1, 2) have been illuminated by a Yag Laser and recorded by two double frame cameras mounted on Scheimpflug mounts. Prisms placed against the channel reduce the optical aberration. For the stereoscopic PIV, the 2C PIV is evaluated by an adaptive multi pass correlation with a window size of 32 by 32 pixels. Then a 3D based calibration method and the pinhole model are used to calculate the three components of the velocity an each field (Calluaud and David, 2004). The 10 Hz frequency of cameras allows following in time the vortex structures and their evolution.

Before the flow measurements, the influence of the laser sheet thickness has been evaluated. A block of resin seeded by solid particles is moved in the three directions and images are recorded for different laser sheet thickness. The accuracy is obtained and the displacement limits for the three component measurements are showed. The figure 2 presents the variations of the average and RMS of the differences between fixed and measured displacements. For block displacements under 1/3 of the laser sheet thickness, measurements stay very accurate (RMS lower than 10 µm). Furthermore, the laser sheet thickness must be adapted to the in-plane spatial resolution of the SPIV measurements. Indeed, no direction must be favoured during the image cross-correlation analysis and 3C SPIV reconstruction. Consequently, by the laser sheet thickness, the out-of-plane resolution is regulated as a function of in-plane spatial resolution. So, for those experiments and in order to have an identical spatial resolution according to three directions, the optimum laser sheet thickness value is about 2 mm.

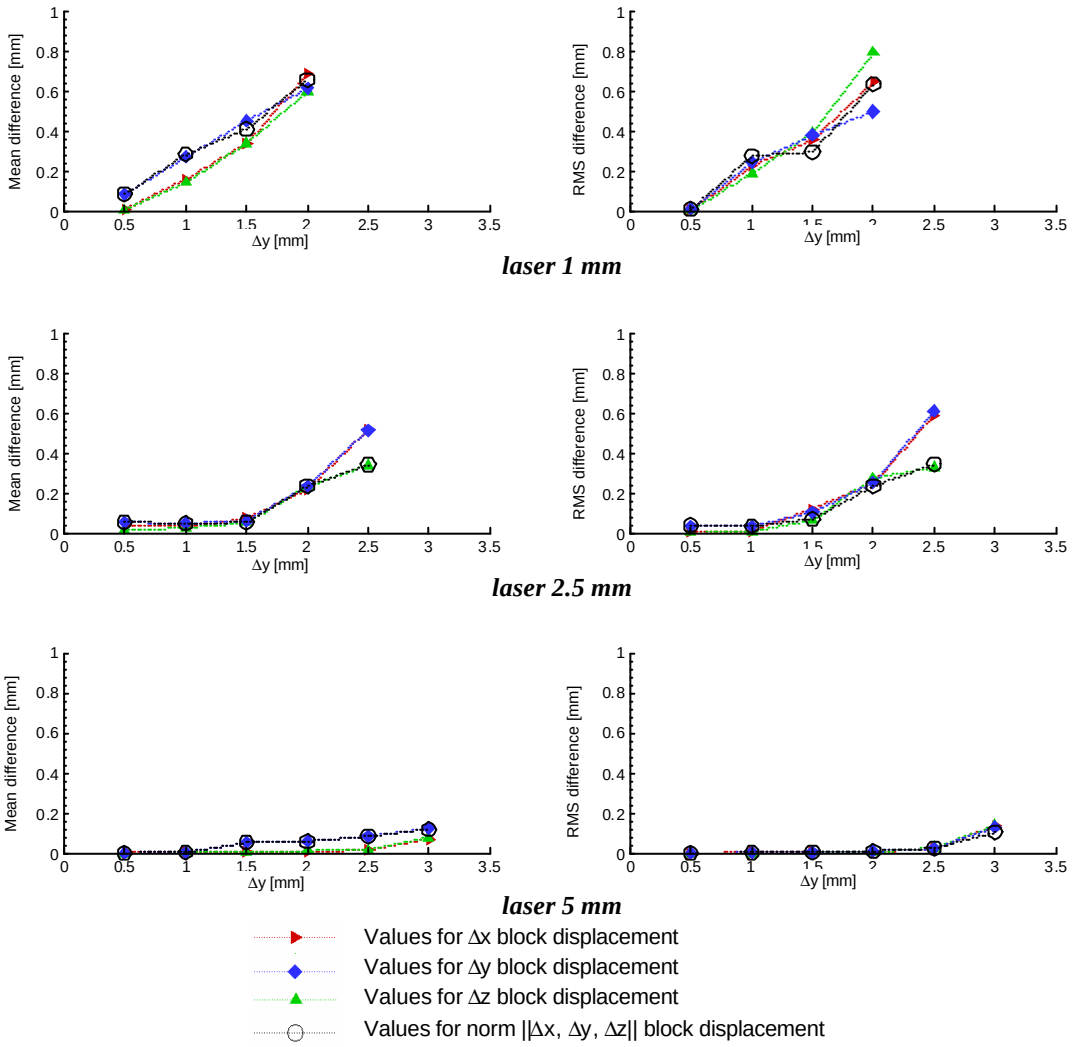

Fig.2 - Real and reconstructed mean and RMS displacement deviations, displayed as a function of the displacement of the block of particles in the direction Z (Dx=Dy= 0 mm), and as a function of laser sheet thickness.

3. Results

Mean velocity aspects are first presented. Instantaneous observations of the kidney vortices in cross-section complete this analysis.

3.1 Mean velocity fields.

The measurements for Re=770 and the different jet-to-cross flow velocity ratio have showed flow topologies and vortex structures highly three-dimensional. The flow is symmetrical in the median section Y/D=0 (fig. 2) and the counter-rotating vortex pair downstream the jet noted CVP appears since X/D=1 (fig.3a and fig.3b) for both cases. These vortices tend to increase along the vertical direction since the flow coming to the upstream region of the jet skirts the jet to limit finally the development of the CVP along the wall. The horseshoe vortex generated upstream the jet by blockage of the fluid for $t_{inj}=0.63$ tends to progress along the width to the section Y/D=1/2 (figure 2d) where it is always visible. For the two others injection velocity, this vortex structure doesn't seem to exist or is blocked inside the hole.
Upstream the jet, the fluid is highly deflected towards exterior according to Y direction. Indeed, downstream, it seems to go up in direction of the central zone by two distinct areas. The first, near Z/D=1, seems to show the roll-up of the CVP structure, and, the second, closer to the wall, is in relation with the wake created downstream the jet by the low pression region between the jet and the accelerated flow on sides.
The influence of the injection's rate is emphasised on the size of CVP vortex. Those always exist for lower injection's rates but are confined downstream the jet (figures 3d and 3f). The recirculation region between these two vortices and the plate tends to be reduced for disappearing for the weakest injection's rate. This phenomenon is confirmed by the disappearance of the negative longitudinal components of the velocity in the sections X/D = 1 and 2, on figures 3c, 3d, 3e and 3f.

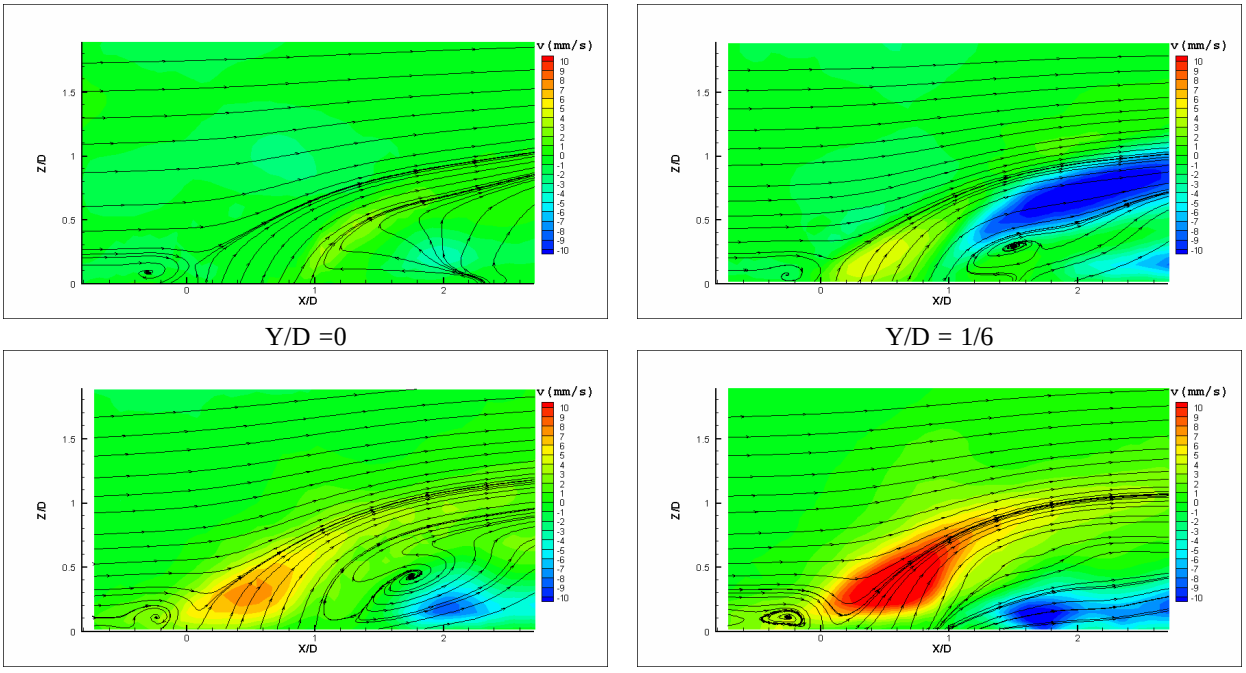

Y/D =0 Y/D = 1/6

Y/D = 1/3 Y/D=1/2

Fig 3: Mean velocity and streamlines for Re=770, t_{inj} =0.63 for Y sections.

3.2 Instantaneous velocity analysis

The analysis of the instantaneous velocity fields shows the difference vortex structures visible in different planes. The horseshoe vortex seems to stay stationary and the fluid above this vortex is deflected. In the near wake, the shear between the jet and the wake downstream the injection creates vortex structures which are shedding with a frequency of about 0.6 Hz. Near X/D=2, the flow is strongly deviated to the top during the shedding process. This section reveals the organization and the modification with time of the kidney vortices.
For the low injection rate, the counter-rotating vortex pair stays steady and their centres are localized near (-0.5;0.5) and (0.5;0.5). For the medium rate (τ_{inj}=0.31), the size of the vortices, their position and orientation vary. The vortex tubes move in spiral with a frequency identical to the vortex shedding frequency generated

downstream the jet. The scheme of the figure 5.b shows the rotation of the main axis of the vortices during the rollup. For the high injection rate, two counter-rotating vortex pairs are generated and merged together during the vortex shedding. The second pair of the CVP appears above the first pair and goes down slowly along trajectories near Y/D=± 1. For each side, the vortices which turn in the same direction merge together and the resulting vortex moved to the section Y/D=±0.4. Then the next merging starts again.

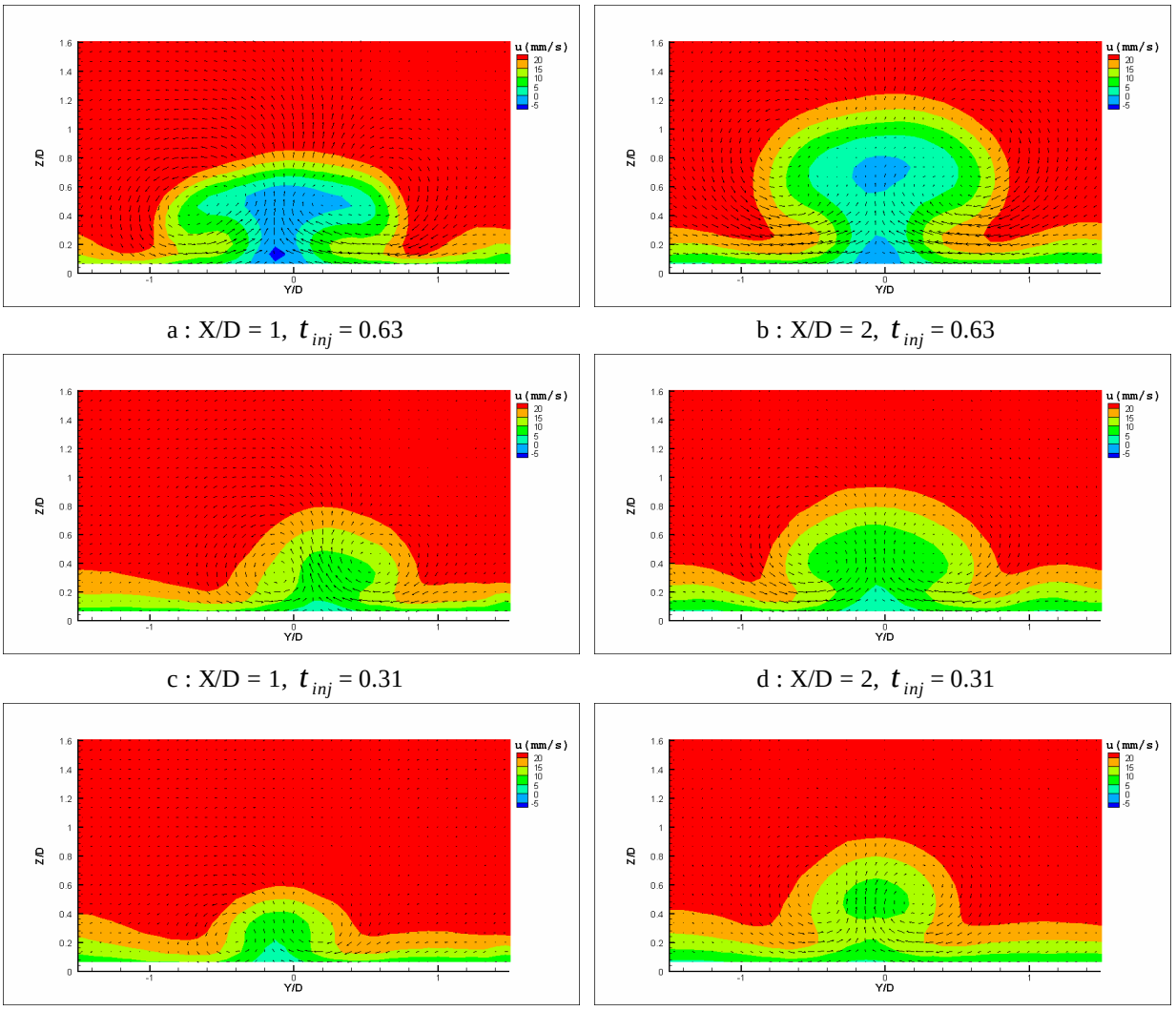

a : X/D = 1, t_{inj} = 0.63 b : X/D = 2, t_{inj} = 0.63

c : X/D = 1, t_{inj} = 0.31 d : X/D = 2, t_{inj} = 0.31

e : X/D = 1, t_{inj} = 0.15 f : X/D = 2, t_{inj} = 0.15

Fig.4: Mean velocity fields for X/D=1 and 2; Re=770, t_{inj} =0.63, 0.31, 0.15

4. Conclusion

In this paper, first results of the study of the perpendicular fluid injection through a square orifice in a cross flow are presented. Stereoscopic Particle Image Velocimetry measurements in sections perpendicular to the main flow have been realized and optimized to obtain a homogenous spatial resolution. The average velocity measurements have allowed to characterize the main aspect of the flow for a Reynolds number of 770 and different injection velocity rates.

A horseshoe vortex structure is present for the highest jet velocity and disappears for the weaker. Downstream the injection, shear between the jet and the near wake creates horizontal axis vortex structures which are shedding regularly. Most of new information appears in the cross-section for X/D= 1 and 2. The well known kidney vortex appears unsteady and composed for τ_{inj}=0.63 by two counter-rotating vortex pairs which merge at the frequency of the shedding observed in sections Y/D. This result confirms those obtained by Haven and Kurosaka for a square injection. For the two other injection rates, only one CVP exists and moves for τ_{inj}=0.31 in a spiral rollup. The vorticity of the flow in the different sections will be now observed in details to complete and explain the formation of these two pairs of vortices.

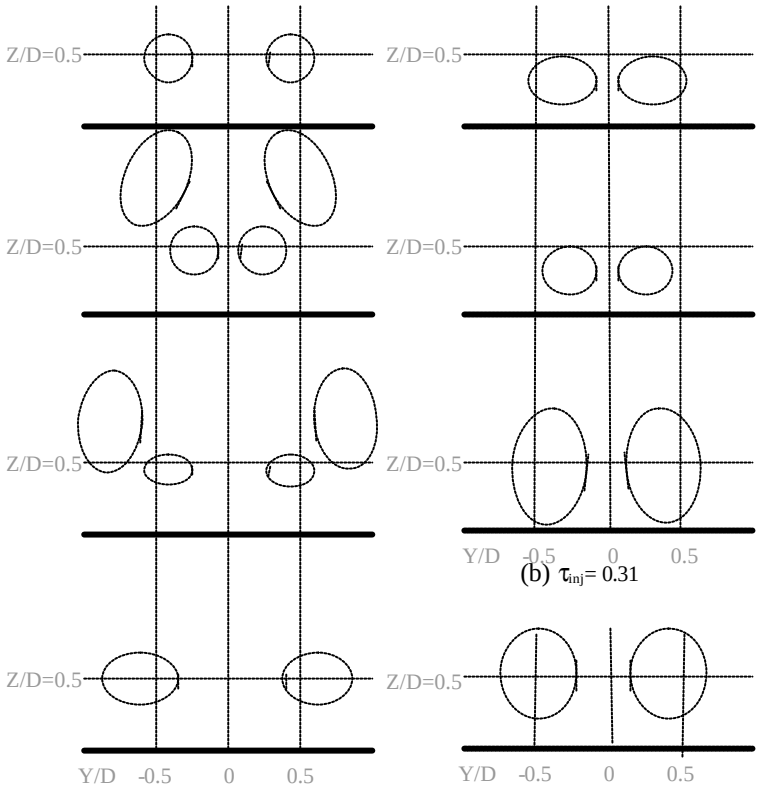

Fig. 5: Kidney vortices for section X/D=2 and different injection rates.

5. References

Andreopoulos J., Rodi W., 1984: Experimental investigation of jets in a crossflow. J. Fluid Mech. vol 183, 93-127.

Brahmi L., Vietoris T.,Rouvreau S., Joulain P., David L., Torero J.L., 2004: The effect of fuel injection on a laminar diffusion flame established on perpendicular fuel and oxidizer streams. Submitted in *Combustion and Flame*.

Calluaud D., David L., 2004: Stereoscopic Particle Image Velocimetry measurements of the flow around a surface mounted block., *Experiments in Fluids.*

Fric T.F., Roshko A., 1994: Vortical structure in the wake of a transverse jet. J. Fluid Mech. Vol 279, 1-47.

Haven B.A., Kurosaka M., 1997: Kidney and anti-kidney vortices in crossflow jets. J. Fluid Mech., vol 352, 27-64.